ACS SyntheticBiology

pubs.acs.org/synthbio

Research Article

Bacteria Engineered to Produce Serotonin Modulate Host Intestinal Physiology

Chrystal F. Mavros,[▽] Mareike Bongers,[▽] Frederik B. F. Neergaard,[▽] Frank Cusimano, Yiwei Sun, Andrew Kaufman, Miles Richardson, Susanne Kammler, Mette Kristensen, Morten O. A. Sommer,* and Harris H. Wang*

Cite This: *ACS Synth. Biol.* 2024, 13, 4002–4014

Read Online

ACCESS | Metrics & More | Article Recommendations | Supporting Information

ABSTRACT: Bacteria in the gastrointestinal tract play a crucial role in intestinal motility, homeostasis, and dysfunction. Unraveling the mechanisms by which microbes impact the host poses many challenges due to the extensive array of metabolites produced or metabolized by bacteria in the gut. Here, we describe the engineering of a gut commensal bacterium, *Escherichia coli* Nissle 1917, to biosynthesize the human metabolite serotonin for examining the effects of microbially produced biogenic amines on host physiology. Upon oral administration to mice, our engineered bacteria reach the large intestine, where they produce serotonin. Mice treated with serotonin-producing bacteria exhibited biological changes in the gut at transcriptional and physiological levels. This work establishes a novel framework employing engineered bacteria to modulate luminal serotonin levels and suggests potential clinical applications of modified microbial therapeutics to address gut disorders in humans.

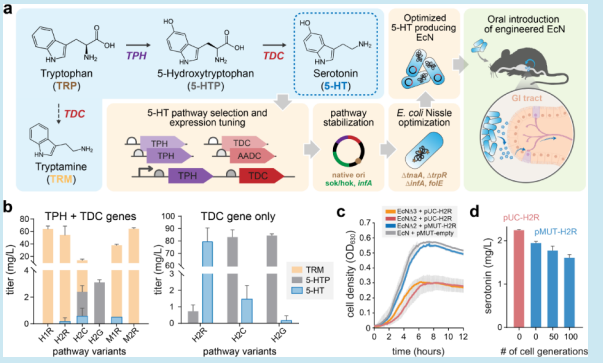

KEYWORDS: *E. coli Nissle 1917, 5-HT, serotonin, microbiome engineering, engineered probiotic, gut-brain*

INTRODUCTION

Intestinal bacteria play a pivotal role in metabolizing foods, influencing host immune responses, and generating various bioactive chemicals that collectively contribute to the maintenance of gastrointestinal (GI) health and homeostasis.[1] There is increasing recognition that gut microbes are involved in bidirectional signaling with the enteric nervous system (ENS) and central nervous system (CNS) along the microbiota−gut−brain (MGB) axis.[2] Oral ingestion of certain probiotic bacteria that produce γ-aminobutyric acid (GABA) can alter host physiology and behavior in animal models,[3,4] which suggests a potential link between gut microbiota and host neurons. On the other hand, psychological stress can induce gut microbiome dysbiosis.[5−7] Strategies to tune specific gut metabolites *in vivo* could better help dissect the mechanistic pathways of the MGB axis.

An essential neurotransmitter involved in signaling throughout the human body is the biogenic monoamine serotonin (5-hydroxytryptamine, 5-HT), with up to 95% of its production occurring in the GI tract.[8] Gut-derived serotonin modulates a vary of functions including intestinal motility, cell turnover, and gut homeostasis.[1,9] Host serotonin synthesis involves a two-step pathway, which starts with hydroxylation of tryptophan (TRP) by a tryptophan hydroxylase (TPH) to form the intermediate 5-hydroxytryptophan (5-HTP) and it is subsequently decarboxylated by tryptophan decarboxylase (TDC) to yield 5-HT. Serotonin levels can be altered with selective-serotonin reuptake inhibitors (SSRIs), which has been used extensively to treat depression, but suffers from negative GI manifestations[10] and serotonin syndrome due to toxic accumulation of excess peripheral 5-HT.[11] Recent studies have shown that commensal bacteria can stimulate host serotonin production *ex vivo*[12,13] and in animals through TPH1 activation[13,14] and downregulation of monoamine oxidase A (MAOA),[15] which plays a key role in the catabolism of serotonin. However, our understanding of intestinal 5-HT homeostasis and the relationship between gut-derived and CNS serotonin remain incomplete. The ability to produce 5-HT directly by bacteria in the gut could provide an avenue to improve the control of serotonin-associated functions in the gut and systemically. This has previously been demonstrated in a loperamide-induced constipation mouse model, where intestinal motility was restored by an engineered bacterium delivering 5-HT *in vivo*.[16]

Received: June 25, 2024
Revised: November 6, 2024
Accepted: November 8, 2024
Published: November 27, 2024

https://doi.org/10.1021/acssynbio.4c00453
ACS Synth. Biol. 2024, 13, 4002−4014

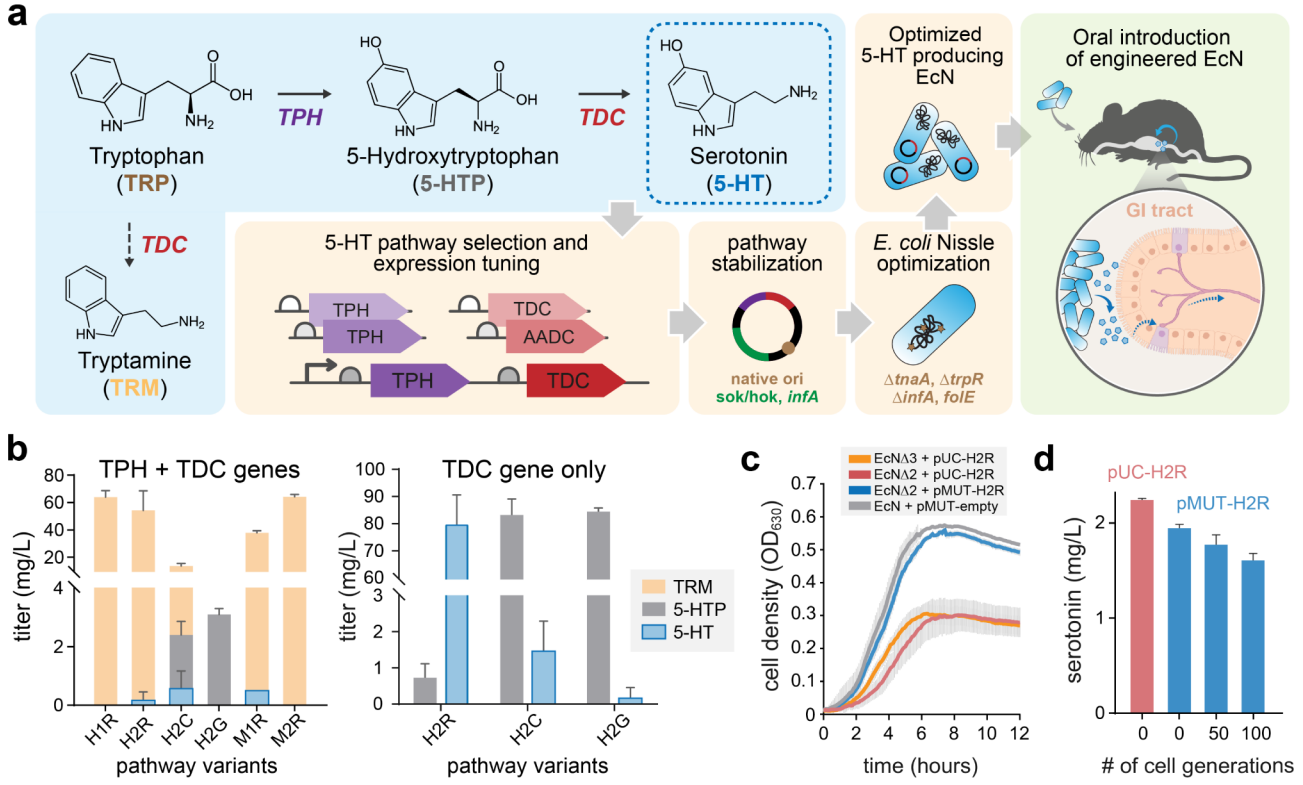

Figure 1. Overview of methods for engineering and characterization of serotonin-producing bacteria. (a) Overall study design to engineer a serotonin (5-HT) biosynthetic pathway into *E. coli* Nissle 1917 and to optimize production in the GI tract to modulate host physiology. (b) Characterization of serotonin production pathways using different eukaryotic tryptophan hydroxylase (TPH) and tryptophan decarboxylase (TDC) genes. Combinations of *TPH* (M1, M2, H1, and H2) and *TDC* (R, C, and G) genes expressed from a high copy plasmid in NΔ2. Feeding tryptophan to test the TPH step resulted in 5-HTP and serotonin (5-HT) production from pathways "H2R", "H2C", and "M1R" (left panel). Feeding the substrate 5-HTP to TDC showed that all enzymes produced serotonin, with the TDC from rice "R" giving the highest conversion (right panel). (c) Transferring the 5-HT pathway from a high copy pUC vector to the native EcN plasmid pMUT1 restored strain fitness to wild-type levels. (d) Stable 5-HT production over 100 cell generations without antibiotic selection for the plasmid. All data shown are mean ± SD (n = 3). 5-HT, 5-hydroxytryptamine (serotonin); 5-HTP, 5-hydroxytryptophan; H1, human TPH1; H2, human TPH2; M1, mouse TPH1; M2, mouse TPH2; C, cataranthus TDC; G, guinea pig TDC; R, rice TDC; RBS, ribosome binding site; TRM, tryptamine; TRP, tryptophan; TDC, tryptophan decarboxylase; TPH, tryptophan hydroxylase.

Advances in synthetic biology and microbial engineering are enabling the development of advanced microbiome therapeutics.[17,18] These engineered microbes can be programmed to diagnose diseased states,[19−22] reduce pathogenic infections,[23] and generate various metabolites, enzymes, and biologics within the gut.[24−27] Many drugs suffer from instability, degradation, and off-target absorption during oral delivery. *In situ* production of these therapeutic compounds at the site of maximal therapeutic effect could greatly improve their bioavailability and potency in the gut. However, safety and reproducibility of live bacterial therapeutics remain challenging in the context of heterogeneous gut microbiome backgrounds across people.

Here, we describe the engineering of a probiotic *Escherichia coli* to biosynthesize serotonin in the mammalian GI tract. We show in a murine model that oral administration of this serotonin-producing bacteria altered host gut physiology, including changes in circadian rhythm-dependent GI motility and intestinal gene expression. This study demonstrates modulation of gut luminal serotonin using an engineered orally delivered probiotic that could potentially modulate the MGB axis.

RESULTS

Engineering and Optimization of Serotonin-Producing Gut Bacteria. Considering the physiological importance of serotonin, we aimed to engineer a bacterium capable of 5-HT production in the gut (Figure 1a). To the best of our knowledge, no bacterial genes have been found to biosynthesize serotonin *de novo*. Consequently, heterologous 5-HT production requires eukaryotic biosynthetic enzymes and thus faces key obstacles for gene, pathway, and host selection. TPH requires molecular oxygen, which is limited in the GI tract, ruling out strict anaerobes as microbial hosts. 5-HT enzymes can often be promiscuous, resulting in side-products such as tryptamine (TRM) that reduce 5-HT yield. Non-native cofactors are often required to support sustained 5-HT biosynthesis. The optimal operating temperature should be the 37 °C gut environment, which preclude some enzymes such as plant cytochrome-P450 tryptamine monooxygenases that operate at 20 °C.[28] Two-step fermentation processes can improve 5-HT production but they cannot be feasibly implemented *in situ* in the GI.[29]

We chose *Escherichia coli* Nissle 1917 (EcN) as the bacterial chassis strain for 5-HT pathway engineering because of its long history as a safe probiotic in humans,[30] and its recent use as an engineered live therapeutic in the GI tract.[24,25] We first tested

https://doi.org/10.1021/acssynbio.4c00453
ACS Synth. Biol. 2024, 13, 4002−4014

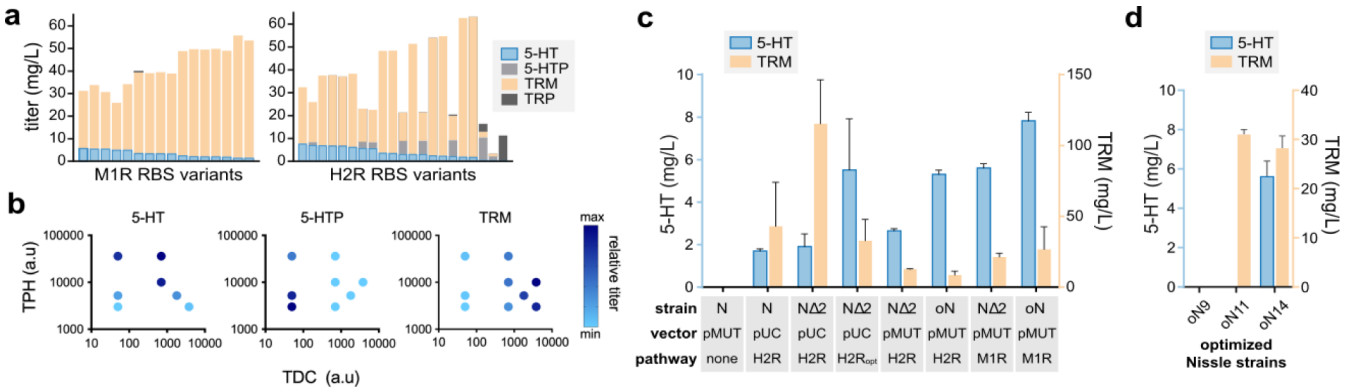

Figure 2. Optimization of serotonin-producing bacteria. (a) Optimization of pMUT-H2R and pMUT-M1R plasmids in oN by combinatorial testing the relative expression levels of *TPH* and *TDC* through the change of RBS variants, represented are stacked bar-plots of the measured metabolites. Data shown are mean (n = 3). (b) Relative titer levels for 5-HT, 5-HTP, and TRM, from corresponding RBS strengths for "H2R" pathway; y-axis TPH, x-axis TDC; as translation initiation rate (a.u). Data shown are mean (n = 3). (c) Sequential engineering steps to optimize serotonin production. Initial EcN wild-type + pUC-H2R, followed by introduction of the knockout of trpR and tnaA (NΔ2). Lowering the RBS and codon optimizing the TDC (pUC-H2Ropt) improved serotonin yield while lowering the yield of tryptamine. Pathway transfer from a pUC to a pMUT1-based plasmid reduced titers, but the mutation in the *folE* gene (oN) restored serotonin production. The highest 5-HT titer (7.8 mg/L ± 0.4) was achieved from the plasmid pMUT-M1R in the oN strain. Data shown are mean ± SD (n = 3). (d) Final strains for *in vivo* testing were derived from oN + pMUT-M1R and show either no (oN9: oN + pMUT09-ctrl), tryptamine only (oN11: oN + pMUT11-trm) or serotonin and tryptamine (oN14: oN with pMUT14-ser) production *in vitro*. Data shown are mean ± SD (n = 3).

different *TPH* and *TDC* genes cloned on a high-copy pUC plasmid in EcN to establish a synthetic serotonin pathway from TRP to 5-HTP and then to 5-HT. The hydroxylation step was tested under tryptophan supplementation in combination with TDC from rice (R), as well as the *TPH2* (H2) in combination with guinea pig (G) or *Catharanthus roseus* (C). We found measurable 5-HTP and serotonin using the mouse *TPH1* (M1) or human *TPH2* (H2), while none where observed from mouse *TPH2* (M2) or human *TPH1* (H1) (Figure 1b). When the decarboxylation step was tested, feeding 5-HTP, for the pathways H2R, H2C, or H2G, we found that TDC from rice was superior for production of serotonin (79.5 mg/L ± 11.1% yield) (Figure 1b). We therefore focused further optimizations on the H2R and M1R pathways. Since increasing the availability of TRP can increase pathway yield for H2R (Figure S1a), we increased the tryptophan pathway flux by knocking out the tryptophan repressor *trpR* and tryptophanase *tnaA* in EcN. A green fluorescent protein (*GFP*) gene were integrated into the Tn7 site of the genome to facilitate easy detection, generating the more optimized base strain NΔ2 (Δ*trpR*, Δ*tnaA*, attTn7:*GFP*).

To enable efficient and iterative optimization of the synthetic 5-HT pathway, plasmid-based expression is preferable. However, for *in vivo* applications, it is undesirable to use antibiotic selective pressure for plasmid maintenance and to have the possibility of the horizontal transfer of plasmids to other resident microbes. To address this challenge, we first attempted to stabilize the high copy number 5-HT production plasmid (pUC-H2R) by introducing the essential bacterial gene *infA* into the pathway operon, and then knocking out the genomic copy in EcN.[31] While stable, this plasmid caused an undesired growth defect in both NΔ2 and NΔ3 (EcN with Δ*trpR*, Δ*tnaA*, and Δ*infA*), likely due to metabolic burden (Figure 1c). We therefore explored an alternative approach by moving the pathway to one of the two native plasmids in EcN, pMUT1.[32] We found that this plasmid (pMUT-H2R) was stably maintained in NΔ2 with no detectable fitness defect for at least 100 generations, without antibiotic selection (Figures 1d and S1b,c). 5-HT production was stable over this period and comparable to that of pUC-H2R titers (Figure 1d). To further ensure plasmid stability *in vivo*, we introduced the *hok/sok* toxin-antitoxin module[33] into subsequent versions of the pMUT plasmids.

Plant TDC enzymes can promiscuously use both TRP and 5-HTP as substrates to generate TRM and 5-HT, respectively.[34−36] To reduce TRM byproduct and redirect the metabolic flux toward 5-HT, we improved the catalytic activity of TPH by introducing a genomic mutation (T198I) in *folE* to increase the conversion of GTP to dihydroneopterin 3′-triphosphate, which catalyzes the first committed precursor toward increased availability of tetrahydromonapterin a native cofactor for pterin-dependent hydroxylation.[37,38] With this improvement, we took this optimized strain (called oN, for "optimized Nissle") and used it combinatorially to test the relative expression strength of *TPH* and *TDC* with ribosome binding site (RBS) libraries for both the "M1R" and "H2R" pathways (Figures 2a−c, S1d and Table S1). Increased 5-HT production was obtained with relative strength of the RBS of TPH exceeding that of TDC, indicating a balance between the two enzymes' relative translation is needed to reduce TRM formation, while avoiding accumulation of the intermediate 5-HTP. Given the limited oxygen availability in the gut and the higher oxygen-binding capacity of *TPH1* than *TPH2*,[39] we elected to use the "M1R" variant with the highest serotonin production as the final pathway (pMUT14-ser), which was put into NΔ2. This final optimized strain (oN14) had superior performance compared to all other combinations of strains, vectors, and pathways tested (Figure 2c). Since tryptamine is known to modulate serotonergic pathways and activate serotonin receptors in the gut,[40] we also built a construct (pMUT11-trm), which lacks the *TPH* gene and thus exclusively produced tryptamine, in order to untangle the effects of the TRM byproduct *in vivo*. A strain (oN11) with pMUT11-trm and a strain (oN9) with an empty vector (pMUT) were made as controls (Figures 2d and S1e).

Oral Delivery of Engineered Bacteria and *In Vivo* Serotonin Production. To test our engineered strains *in vivo*, we used 6-week-old conventional C57BL6/J mice (Taconic

https://doi.org/10.1021/acssynbio.4c00453
ACS Synth. Biol. 2024, 13, 4002−4014

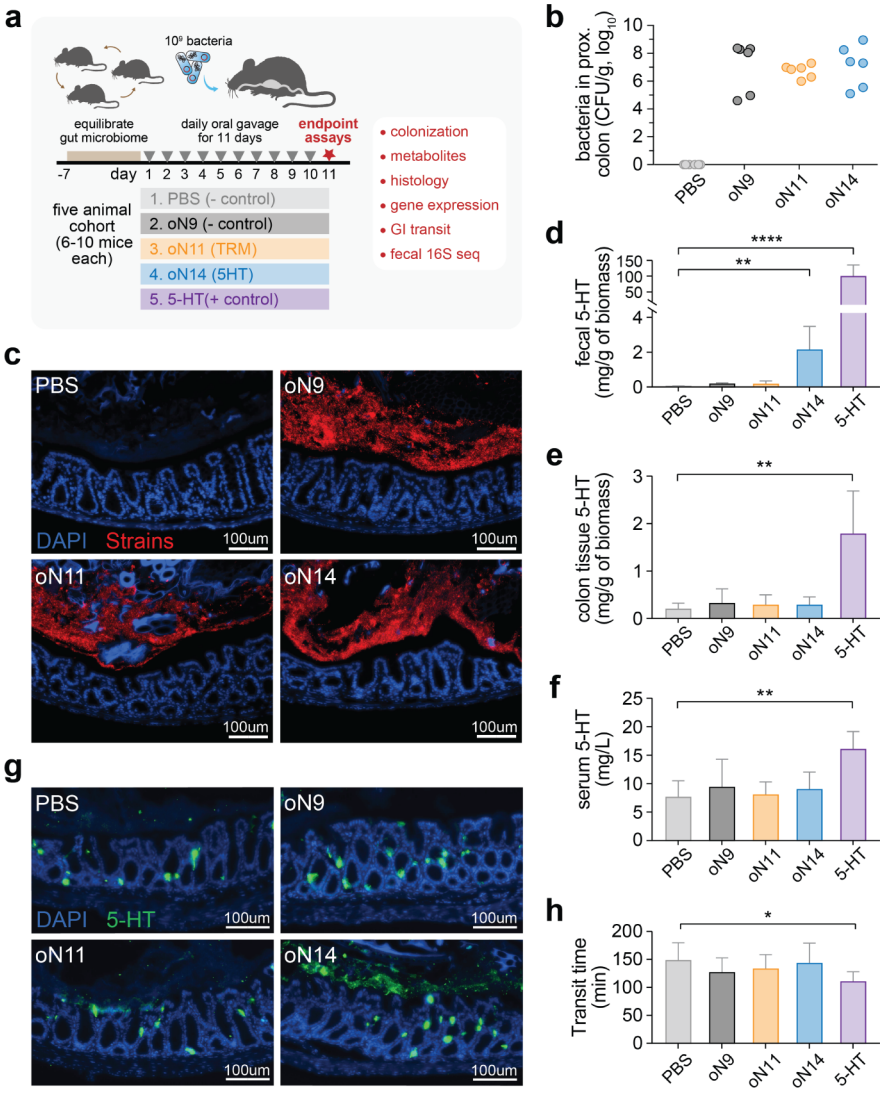

Figure 3. Changes in host physiology and *in vivo* metabolite concentrations induced by serotonin supplementation. (a) Schematic of experimental paradigm from mice orally supplemented with PBS, oN9, oN11, oN14, or 5-HT (1.5 mg/mL). (b) Concentration of engineered strains in the proximal colon, which is the most densely populated region 24 h after the last gavage. Colonies on LB + kanamycin plates, measured as colony forming units (CFU) per gram of fecal matter, are shown (n = 6). (c) Immunohistochemical staining with anti-green fluorescent protein (GFP) antibody in a section of the mid colon, with a scale bar of 100 μm. (d–f) Serotonin concentration in the feces, cleaned homogenized colon tissue, and serum (respectively) (n = 8, one-way ANOVA on ranks). (g) Immunohistochemical staining with antiserotonin antibody in the midcolon, with a scale bar of 100 μm. (h) Total gastrointestinal transit time from mouth to anus using a 6% Carmine red solution, performed at start of light cycle (7 AM) (n = 8, one-way ANOVA on ranks). Data are mean values with error bars as standard deviation. *p < 0.05, **p < 0.01, ***p < 0.001, and ****p < 0.0001.

Biosciences). Mice underwent a 7-day microbiome normalization protocol in which their bedding was homogenized and redispersed daily, which reduced intercage microbiome variation. Subsequently, mice were divided into separate groups and orally gavaged with 10^9 colony-forming units (CFUs) of freshly grown cultures of oN9, oN11, oN14 (henceforth referred to as "oN strains") sterile phosphate-buffered solution (PBS), or 1.5 mg/mL 5-HT in PBS, daily for 11 days (Figure 3a). The mice gavaged with 5-HT also received the compound in their drinking water. 24 h after the last gavage, the mice were euthanized to acquire intestinal digesta, blood serum, and colon tissues for further analysis.

We first assessed the short-term colonization and localization of strains along the GI tract by plating the digesta derived from different intestinal regions (Figure S2a) and quantified the number of GFP-positive, kanamycin resistant (KanR) colonies (Figure S2b). The highest concentration of oN was found in the proximal colon at more than 10^8 CFU/g (Figure 3b), localizing along the mucosal layer based on visualization by immunohistochemistry with an anti-GFP antibody (Figure 3c). In contrast, the small intestine had much fewer oN bacteria (<10^4 CFUs/g) compared to the cecum or colon (Figure S2b). Therefore, during our 11-day oral administration protocol, the oN strains appear to primarily accumulate in the large intestine near the epithelial lining compared with other GI regions. To verify the maintenance of the engineered plasmid and serotonin production capacity after passing through the GI tract, we isolated oN14 colonies recovered from feces and profiled for 5-HT production, which showed consistent serotonin levels compared to the initial inoculum (Figure S2c).

https://doi.org/10.1021/acssynbio.4c00453
ACS Synth. Biol. 2024, 13, 4002–4014

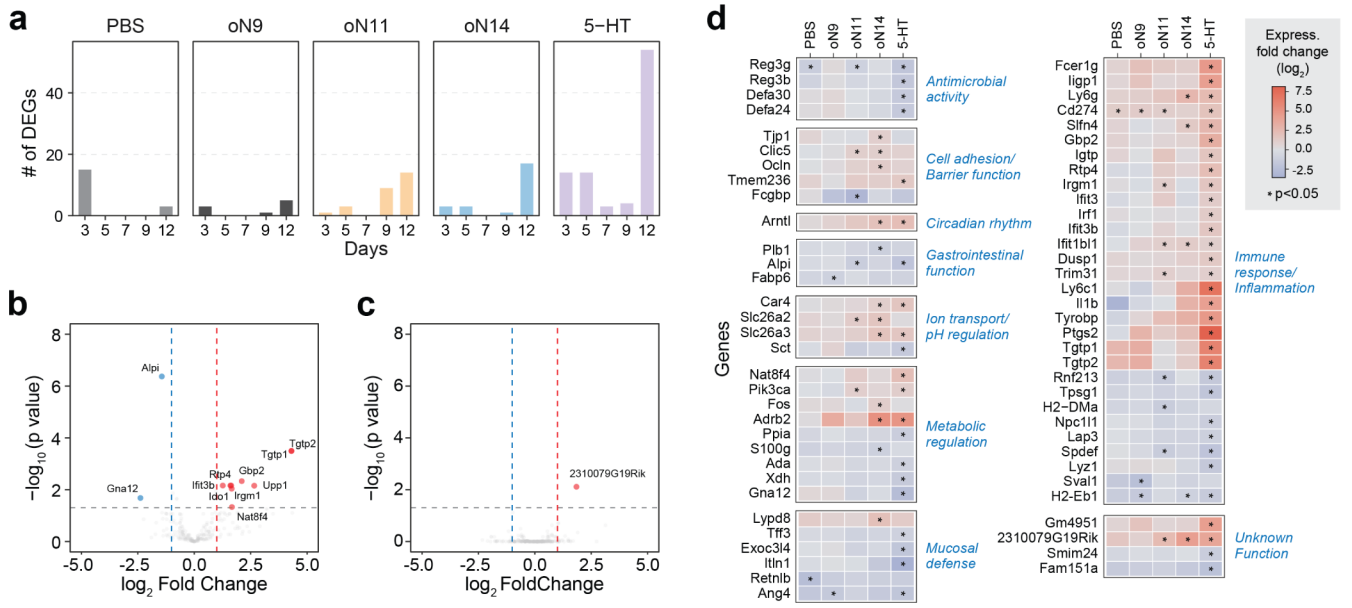

Figure 4. Transcriptomic profiling and Gene Ontology annotation of associated functional categories. (a) Number of differentially expressed genes (DEGs) for each treatment group at each time point, compared to day 1. Volcano plot of DEGs identified between PBS/5-HT groups in (b) and oN9/oN14 groups in (c). Blue dots denote down-regulated gene expression, red dots denote up-regulated gene expression, and gray dots denote gene expression without marked differences. (d) Heatmap showing expression profiles of significant DEGs from day 0 vs day 12 (per subject, averaged within treatment groups) and associated functional categories. Significant values are shown with an asterisk (*) for $p_{adj} < 0.05$ and abs(fold change) > 2.

We next probed for evidence of 5-HT production in the murine gut from the oN14 strain by measuring fecal 5-HT using an ELISA assay. A significant increase ($p < 0.01$ by ANOVA) in fecal 5-HT was observed in mice given the serotonin-producing strain oN14 or the positive control, oral 5-HT (Figure 3d). Although the oN14 levels were not as high as those from direct oral 5-HT administration, these findings demonstrate the *in vivo* production of 5-HT by the oN14 strain. To explore the systemic and tissue-specific distribution of 5-HT, we measured 5-HT presence in serum and colonic tissues. Significant increases ($p < 0.01$ by ANOVA) in colonic and serum 5-HT were observed in the 5-HT group only (Figure 3e,f). These results demonstrate that high levels of luminal 5-HT can cross from the gut into the blood, where it normally accumulates in the platelets. Excess 5-HT in platelets can result in increased serum serotonin levels observed in the 5-HT group. Since 5-HT levels were not elevated in colonic tissues that have been cleaned to remove residual digesta in the oN14 group, which could be attributed to absorption competition of the serotonin transporters (SERT) with the site product TRM.[41] We speculated that serotonin may be more concentrated in the mucosal layers, where oN strains are observed. To test this hypothesis, we stained for 5-HT in whole-paraffin-embedded colonic sections using an antiserotonin antibody and visualized the distribution along the mucosa (Figure 3g). Indeed, we found that serotonin was enriched along the mucosal layers specifically in the oN14 group compared with oN9 or oN11. Taken together, these results show that the engineered oN14 strain produces 5-HT *in vivo* along the mucosa of the murine colon but 5-HT does not reach circulation in detectable amounts.

Impact of Luminal Serotonin on Host Gut Physiology, Microbiome, and Gene Expression. Serotonin is recognized for its role in modulating GI motility, triggering intraluminal pressure that induces peristaltic reflexes and colonic migrating motor complexes during fasting intervals.[42,43] To first explore whether this response exhibits temporal rhythmicity aligned with circadian rhythm, we investigated the impact of oral 5-HT supplementation on gut transit at two distinct times: 7AM (commencement of the light cycle) and 7PM (commencement of the dark cycle). Oral serotonin supplementation (1.5 mg/mL) over an 11-day period accelerated morning gut motility but did not influence motility in the evening (Figure S3a,b). Consequently, these results prompted us to test oN strains specifically in the morning in subsequent experiments. However, we observed no changes in GI motility in mice administered oN9, oN11, or oN14 compared to oral 5-HT, which showed a significant speed up in transit time (Figure 3h). The absence of transit time changes in oN strains suggests that the lower level of serotonin production by oN14 may be insufficient to influence gut motility. Another factor is that 5-HT presence in the small intestine in the oral 5-HT cohort may more dramatically affect gut motility, whereas detectable 5-HT production by oN14 likely localizes mostly to the large intestine at the mucosa. Furthermore, we observed no significant changes in weight regardless of treatment group (Figure S3c).

Considering that changes in gut motility and exogenous biogenic amines may influence the gut microbiome,[44] we performed 16S metagenomic sequencing on fecal matter across the five animal cohorts at days −7, 1, 3, 5, 7, 9, and 12 (Materials and Methods). We verified that our homogenization protocol between day −7 and day 0 successfully normalized the microbiome between animals, mediating any initial cage-based variation that would likely occur otherwise (Figure S4a). While some global relative abundance shifts were observed for all cohorts (Figure S4b,c), such as reduction of Muribaculaceae by day 12, we did not observe selection for or against any particular taxa as indicated by a generally stable alpha diversity (Figure S4d). We did detect the presence of the

https://doi.org/10.1021/acssynbio.4c00453
ACS Synth. Biol. 2024, 13, 4002−4014

administered EcN strains in stool (Figure S4e). These results indicate that the gut microbiome is not significantly impacted by an increase in exogenous 5-HT in the gut.

To determine whether luminal 5-HT accumulation impacted the gut transcriptome, we evaluated the longitudinal host gene expression changes in the murine gut by RNA sequencing. Transcriptomic analysis revealed up to 53 differentially expressed genes (DEGs) between day 0 and day 12 within each individual animal cohort (Figure 4a). Similar transcriptional changes were observed in the oN14 and oral 5-HT cohort. DEGs associated with host responses to external stimuli based on GO annotation were enriched, particularly those that respond to biotic stimuli, including bacterium recognition, defense responses, and cellular responses to interferon-beta (Figure 4b,c). These changes are likely influenced by serotonin receptor activation of various immune cells.[45] Notably, we did not detect expression changes in Tph1, other genes associated with serotonin metabolism, or other tryptamine derivatives. Given that enterochromaffin cells and other 5-HT-receptor expressing cell types constitute ∼1% of the epithelial cell population,[46,47] serotonin responsive transcriptomic changes may fall below detection.

Of the notable DEGs (Figure 4c), the circadian rhythm gene *Arntl* (*Bmal1*) has been previously linked to changes in serotonin in the CNS,[48,49] suggesting a potential role in enteric neurons. Inflammation-related DEGs, such as *Ly6g* and *Il1b*, were observed in both the 5-HT and oN14 groups, hinting at potentially proinflammatory properties of 5-HT in the GI tract. These changes gradually increased over the time course of the experiment (Figure S5). This suggests that the oN14 strain induces transcriptional changes comparable to those of direct 5-HT administration, indicating local delivery of 5-HT *in vivo*. Nevertheless, further examination is needed to elucidate the precise interaction between the host and elevated serotonin levels throughout the gut lumen. Collectively, these findings highlight that our engineered bacteria elicit several changes in the gut, including host gene expression and GI motility, without disturbing the resident microbial community.

DISCUSSION

The role of 5-HT and its relationship between gut-derived and CNS-derived signals are yet to be fully elucidated. The majority of peripheral 5-HT, produced by enterochromaffin cells in the intestinal mucosa, serves as a modulator of gastrointestinal function through paracrine signaling as well as influence distant organs and modulate immune responses via endocrine pathways. Furthermore, the intestinal microbiome plays a crucial role in the regulation, production, and release of serotonin, affecting both lateral and luminal secretion. This study establishes a novel tool for investigating the role of molecular delivery in intestine function by genetically engineering the probiotic strain EcN to deliver serotonin (oN14). We demonstrate thorough engineering of eukaryotic enzymes to enable the biosynthesis of serotonin in EcN, facilitating its synthesis and subsequent delivery under physiologically relevant conditions in the gut environment. This engineered *E. coli* Nissle 1917 strain, oN14, can populate the murine large intestine to a sufficient density to increase the 5-HT in the feces.

Increasing luminal 5-HT levels induced transcriptional changes in the host GI tract, particularly in genes associated with the host's immune response, metabolic regulation, mucosal defense, and circadian rhythm. Many of these changes correspond to serotonin receptor activation of various immune cells. Ion channels, such as the chloride channel SLC26A3,[40,50,51] were modulated in mice given oN14 and 5-HT, respectively, suggesting an indirect response to elevated 5-HT levels consequently accelerating transit time. Furthermore, the increased expression of the β2-adrenergic receptor (Adrb2) by both 5-HT and oN14 implies indirect activation through other neurotransmitters, possibly epinephrine. Of note, changes in Cd274 were observed in mice given oN9, oN11, and 5-HT, but not in animals given oN14. A recent study[52] identified tryptophan as an agonist of PD-L1 (encoded by Cd274) induction, yet this effect was not observed in pancreatic β cells treated with serotonin. Nevertheless, our results suggest a potential role for luminal serotonin in activating the immune pathways in the gut. Mice given oN14, as well as those given 5-HT, exhibited alterations in the circadian rhythm gene *Arntl*, aligning with the observed time-of-day dependence for GI motility. Using a loperamide-induced constipation model, another group was able to revert the transit time to baseline with a genetically modified (minimally described) 5-HT producing EcN.[16] In contrast, we observed no alteration in the healthy microbiome, but direct comparisons are challenging due to differences in study design and models, and potential vendor specific variation in the microbiome.[53]

Employing genetically programmable gut-colonizing bacteria, circumventing the need for antibiotics or germ-free models, paves the way for the study of bacterially produced metabolites under physiologically relevant conditions. This approach will enable future research aimed at elucidating the role of gut-derived metabolites in host physiology and their broader systemic effects. The use of engineered commensal bacteria that target specific regions of the GI tract can enhance the specificity and efficacy of various pharmacological compounds, particularly those that present challenges in oral formulation and administration. While current serotonin-modulating therapeutics alter serotonergic signaling via established 5-HT receptors and transporters, these can cause adverse systemic effects, such as serotonin syndrome. Our oN14 strain enables targeted colonic delivery of 5-HT, overcoming the hurdles associated with oral administration due to inherent instability. However, our findings suggest that intestinal serotonin triggers immune responses that contribute to inflammatory pathways. Therefore, further research is necessary to understand the impact of long-term serotonin-based therapies on both intestinal and systemic health, particularly in the context of inflammatory conditions. Both elevated and reduced 5-HT levels have been reported in patients with inflammatory bowel disease (IBD), indicating that the role of luminal 5-HT in disease pathology remains unclear and requires further investigation.[54] However, intestinal inflammation has been observed in some Crohn's disease (CD) patients with increased levels of 5-HT.[55] The findings presented here, along with the emerging literature[19,23−26] highlight the potential utility of engineered commensal bacteria in both foundational and translational research. Clinical utility of our approach will require meticulous calibration of dosage, treatment duration, and tolerability of engineered bacteria in human subjects to ensure safety and therapeutic success.

https://doi.org/10.1021/acssynbio.4c00453
ACS Synth. Biol. 2024, 13, 4002−4014

MATERIALS AND METHODS

Strain Construction. *E. coli* Nissle 1917 (Mutaflor) was purchased from Ardeypharm GmbH, Germany. The gene for green fluorescent protein (GFP, GenBank: CAH64882.1) was placed under control of a strong, constitutive promoter (Part BBa_J23101, Registry of Standard Biological Parts, www.parts.igem.org) and integrated into the genome at the Tn7 attachment site using pGRG25. Knockouts of *trpR*, *tnaA*, or *infA* were performed using CRISPR/Cas9. Briefly, a two-plasmid system consisting of an inducible cas9/λ-Red expression plasmid and a guide RNA (gRNA) plasmid were used to introduce double-strand breaks at the desired genomic loci. gRNAs were designed using CRISPy-web after uploading the EcN genome sequence (GenBank: CP007799.1). Templates for homologous recombination at the cut site were generated as follows: where available, strains with the desired knockouts (Δ*trpR*:FRT-*kan*-FRT or Δ*tnaA*:FRT-*kan*-FRT, respectively) from the KEIO collection were transformed with pSIJ8 and the FLP recombinase gene was induced to remove the kanamycin resistance gene. Resulting colonies were screened for kanamycin sensitivity. The Δ*trpR*:FRT or Δ*tnaA*:FRT loci were amplified using oligonucleotides binding 500 bp upstream and downstream of the FRT site to generate PCR products of approximately 1 kb. For *infA*, the fragment was generated by first amplifying 500 bp upstream and 500 bp downstream of *infA* from the EcN genome and then fusing these 2 fragments using overlap-extension PCR. For the *folE*(T198I) genomic mutation, the *folE* gene was amplified in 2 parts, introducing the T198I mutation in the oligonucleotides used for the overlap-extension PCR. The resulting dsDNA fragments were purified and cotransformed with the gRNA plasmid to generate markerless gene knockouts or mutations in EcN. CRISPR/Cas9 and gRNA expression plasmids were cured from the strains. In the case of *infA*, plasmid pUC-H2R$_D$ which expresses a synthetic *infA* gene (see below) was transformed into NΔ2 before the CRISPR experiment, to provide a functional copy of the *infA* gene for survival. All genome modifications were verified by using Sanger sequencing.

Serotonin Production Genes and Plasmids. Genes and plasmids used in this study are listed in Table S1. Genes for serotonin production were selected from mammalian or plant protein sequences, codon-optimized for *E. coli* using the online tool from IDT (idtdna.com/CodonOpt) and synthesized by GeneArt (ThermoFischer Scientific) or ordered as gBlocks from Integrated DNA Technologies, Belgium. Plasmid pUC-H2R was used as a template for generating the pUC series of plasmids. The pathway operon consisted of promoter BBa_J23107, a *TPH* gene, a *TDC* gene, and a synthetic copy of the *infA* gene (Figure S1e). Parts of pUC-H2R were amplified, and the *TPH* and/or *TDC* gene was replaced with alternative genes using Gibson assembly. Plasmid pMUT1 (GenBank: A84793.1) was isolated from wild-type EcN and amplified to serve as the pMUT backbone. Elements that could enable plasmid transfer were removed, and a kanamycin resistance gene and the H2R or M1R operons (without *infA*) were inserted to generate pMUT-H2R or pMUT-M1R, respectively. To generate the plasmid pMUT14-ser, the *hok/sok* toxin-antitoxin plasmid stability element (GenBank: MK134376, Region 58002−58601) was additionally inserted into the pMUT-M1R backbone (Figure S1f). The *TPH* gene was removed from pMUT14-ser to generate pMUT11-trm, and both *TPH* and *TDC* were removed to make pMUT09-ctrl.

Pathway Optimization Using RBS Libraries. RBS strength libraries were designed using the "RBS calculator v1.1" choosing library sizes of 4−6 variants for each gene, ranging in theoretical strength from 50 to 50000 arbitrary units (Table S1). Mutations in the RBS were introduced with oligonucleotides containing degenerate bases using Gibson assembly. Transformants were picked randomly and a representation of the RBSs were sequenced after testing the strains' metabolite production profiles.

***In Vitro* Metabolite Production.** For metabolite production, strains were grown in a modified M9 medium containing 1× M9 salts (M6030, Sigma-Aldrich), 0.2% (w/v) glucose, 0.1% (w/v) casamino acids (Cat.No. C2000, Teknova), 1 mM $MgSO_4$, 50 μM $FeCl_3$, 0.2% (v/v) 2YT medium (composition, see below), and 50 mg/L L-tryptophan unless stated otherwise. Kanamycin was added at a final concentration of 50 mg/L unless stated otherwise. Three single colonies were picked from each strain, grown in 300 μL medium in 96 deep-well plates and shaken at 250 rpm at 37 °C for 16 h. The main culture was inoculated by diluting this preculture 1:100 into fresh medium, and cells were grown for 24 h under the same conditions. Afterward, the culture supernatant was separated from cells using a 0.2 μm pore size filter and frozen at −20 °C until analysis by LC-MS. All data shown are normalized to OD_{630} and presented as mean ± SD from at least 3 biological replicates.

Plasmid Stability Testing. Six single colonies each were picked from strains NΔ2 + pMUT-H2R, NΔ2 + pUC-H2R, NΔ2 + pUC-H2R$_D$, and NΔ3 + pUC-H2R$_D$ and grown in 300 μL of 2YT medium (containing 1.6% (w/v) tryptone, 1% (w/v) yeast extract, and 0.5% (w/v) NaCl) without kanamycin in 96 deep-well plates and shaken at 250 rpm at 37 °C for 24 h. The optical density (OD_{630}) of the cultures was measured, cultures were diluted 1:1000 into fresh medium, and cells were plated on LB−agar plates with and without kanamycin daily, corresponding to approximately 10 doublings every 24h. Colony forming units on LB−agar plates ± kanamycin were counted daily. At time points t = 0, 50, and 100 generations, cultures were diluted 1:100 into the modified M9 medium described above (without kanamycin) and serotonin production was measured as described.

Bacterial Growth Curves. Cells were grown as described under "*In vitro* metabolite production" with the following modifications: after inoculation of the main culture, 200 μL were transferred into a flat-bottom, clear 96-well microtiter plate, and the plate was sealed with a gas-permeable membrane (Z380059, Sigma-Aldrich). Growth was recorded using the BioTek ELx800 plate reader by measuring the optical density at 630 nm every 10 min. Cultures were grown at 37 °C with 700 rpm orbital shaking.

Quantification of *In Vitro* Metabolites by LC-MS. Detection of serotonin, tryptamine, tryptophan and 5-HTP were conducted by liquid chromatography mass spectrometry (LC-MS) measurements on a Dionex UltiMate 3000 UHPLC (Fisher Scientific, San Jose, CA) connected to an Orbitrap Fusion Mass Spectrometer (Thermo Fisher Scientific, San Jose, CA). The system used an Agilent Zorbax Eclipse Plus C_{18} 2.1 × 100 mm^2, 1.8 μm column kept at 35 °C. The flow rate was 0.350 mL/min with 0.1% formic acid (A) and 0.1% formic acid in acetonitrile (B) as mobile phase. The gradient started as 5% B and followed a linear gradient to 35% B over 1.5 min.

https://doi.org/10.1021/acssynbio.4c00453
ACS Synth. Biol. 2024, 13, 4002−4014

This solvent composition was held for 3.5 min after which it was changed immediately to 95% B and held for 1 min. Finally, the gradient was changed to 5% B until 6 min. The sample (1 μL) was passed on to the MS equipped with a heated electrospray ionization source (HESI) in positive-ion mode with sheath gas set to 60 (a.u.), aux gas to 20 (a.u.) and sweep gas to 2 (a.u.). The cone and probe temperature were 380 and 380 °C, respectively, and spray voltage was 3500 V. Scan range was 50 to 500 Da and time between scans was 100 ms. Detection of serotonin (160.07646 ion), tryptamine (144.08158 and 161.10775 ions) and tryptophan (205.09785 ion) were conducted in full scan whereas the 5-HTP detection was carried out after HCD fragmentation (221.09 > 162.05553, 25% HCD CE). Quantification of the compounds was based on calculations from calibration standards analyzed before and after sets of 24 samples. Concentrations were normalized to OD_{600} of bacterial strains. All reagents used were of analytical grade.

Animal Studies and Sample Collections. All animal experiments were performed in compliance with the Columbia University Medical Center IACUC protocol AC-AAAV1460. Male mice (C57BL/6) were purchased from Taconic Biosciences at 6−8 weeks of age. Animals were group-housed on a 12-h light:dark cycle (lights on from 07:00 AM−07:00 PM) at constant temperature with ad libitum access to food and water. Upon delivery, mice were given 1 week to adjust to the new location. Mice then underwent a 7-day, microbiome normalization protocol. On day one of the normalization protocol, mice were randomly mixed across new, clean cages, defining the respective cohorts moving forward (2−3 cages per cohort; 3−5 mice in each cage). On days 2 through 6, mice underwent daily bedding homogenization. Roughly 50 g of bedding from each cage was mixed together in a clean container and then redispersed across the cages. On day 7 of the microbiome normalization protocol, mice began day 0 of the experimental protocol and were placed in new clean cages, retaining the same respective cohorts as were determined on day one of normalization. Mice were housed in groups of 3−5 mice in bottle fed cages, set in designated racks, restricted to PI access only, and opened only under a laminar flow hood. Fecal samples were collected at day zero of the experimental protocol and then mice were orally gavaged every 24 h at the same time of day for 11 days. Mice were gavaged with 200 μL sterile PBS, 1.5 mg/mL 5-HT in sterile PBS (concentration based on calculation from references,[44,56] or freshly grown 10^9 cells of oN9, oN11, or oN14 in sterile PBS. Mice given 5-HT were also maintained on drinking water supplemented with 1.5 mg/mL 5-HT throughout the duration of the experiment. On the 11th day, mice underwent gastrointestinal motility (transit time) testing. Mice were euthanized 24 h after motility testing, and tissues were collected for downstream analysis.

***In Vivo* Metabolite Analysis.** Serum, tissue, and fecal samples were analyzed for serotonin. Blood samples taken via cardiac puncture were collected and spun through serum separator tubes (BD 365967) and serum was retrieved per manufacturer instructions. Serum samples were then flash frozen in liquid nitrogen and saved at −80 °C for downstream analysis. Colon tissue was washed with PBS and placed in 0.9% NaCl and 0.1% ascorbic acid solution and sonicated on ice in 10-s intervals. Fecal samples were weighed and immediately homogenized at 50 mg/mL in ELISA standard buffer supplemented with ascorbic acid. The subsequent supernatants from colon tissue and fecal samples were stored at −80 °C for downstream analysis. Serotonin levels were detected by ELISA according to the manufacturer's instructions (Eagle Biosciences SER39-K01). Readings from tissue samples were normalized to total protein content as detected by a Synergy HT Microplate Reader (Biotek).

***In Vivo E. coli* Nissle Strain Colonization Analysis.** Intestinal tissues were harvested for sectioning and digesta were scraped to determine colony forming units (CFUs) of *E. coli* Nissle. Digesta were weighed, subsequently disrupted in 1 mL of PBS, vortexed, and centrifuged. Supernatant was serially diluted, plated on LB−agar plates supplemented with 50 μg/mL kanamycin, and incubated overnight at 37 °C. Colonies were counted the following morning and expressed as CFU per gram of fecal matter.

Immunohistochemistry Analysis. Colon samples were collected, and 5 mm sections were cut in the midcolon and fixed in either a methanol−Carnoy (60% Methanol, 30% Chloroform, 10% Acetic Acid) solution or 4% paraformaldehyde (PFA) in phosphate-buffered solution (PBS) for 24 h. Fixed samples were then washed three times and stored in 70% ethanol. Samples were kept intact with digesta in the lumen, embedded in paraffin, cut luminally at 4 μm, and either prepped for immunohistochemistry or subjected to hematoxylin and eosin staining. For immunohistochemistry: PFA fixed slides were used for serotonin (5-HT) antibody staining, and methacarn fixed samples were used for Muc2, green fluorescent protein (GFP), and chromogranin A (CgA) antibody staining. All slides were baked for 2 h at 57 °C, deparaffinized in xylene and an ethanol−water gradient, rehydrated, then treated with an antigen retrieval solution of 10 mM sodium citrate, pH 6.0 for 30 min at 90 °C. Slides were blocked for 30 min at room temperature with 5% fetal bovine serum (FBS) in PBS and then incubated with primary antibodies at 4 °C overnight in 5% FBS in PBS. Slides were washed with PBS three times, incubated with secondary antibody for 2 h at room temperature in PBS, washed three times in PBS, incubated with DAPI (4′,6-diamidino-2-phenylindole) at 10 μg/mL for 5 min, washed three times in PBS and mounted using glycerol. Slides stained with primary antibodies preconjugated with Alexa fluorophores did not undergo secondary antibody staining. Antibodies used: anti-GFP rabbit IgG with Alexa Fluor 594 conjugate (Life Technologies A21312). Anti-Muc2 polyclonal rabbit (Santa Cruz Technologies sc-15334). Anti-chromagranin A polyclonal rabbit (Abcam ab15160). Anti-serotonin polyclonal goat (Abcam ab66047). Secondary anti-rabbit Alexa Fluor 568 (Thermo-Scientific Novex a11011). Secondary antigoat IgG Alexa Fluor 488 (Abcam ab150077). All images were taken with Nikon Eclipse Ti2-E inverted microscope system, image conversion, and cell size (particle) analysis performed using NIS-Elements, Advanced Research Software and ImageJ (FIJI) for Macbook version 2.0.0-rc-69/1.52i.

Total Gastrointestinal Motility. Carmine red, which cannot be absorbed from the lumen of the gut, was used to study the total GI transit time. A 6% solution of carmine red (300 μL; Sigma-Aldrich) suspended in 0.5% methylcellulose (Sigma-Aldrich) was administered by gavage through a 21-gauge round-tip feeding needle. The time at which gavage took place was recorded as T_0. After gavage, fecal pellets were monitored at 10 min intervals for the presence of carmine red. Total GI transit time was considered as the interval between T_0 and the time of first observance of carmine red in stool.

https://doi.org/10.1021/acssynbio.4c00453
ACS Synth. Biol. 2024, 13, 4002−4014

Fecal Sample Collection and Homogenization. Fresh mouse fecal pellets were collected into a sterilized Eppendorf 1.5 mL tube and immediately frozen on dry ice. The sample was then transferred to a −80 °C freezer for long-term storage. Prior to sample homogenization, the weight of frozen fecal pellets was determined by using an analytical balance. Next, 1 mL of DNA/RNA shield buffer (Zymo R1100) and 3× sterilized plating glass beads (3 mm) were added to each tube and the fecal sample was then thoroughly homogenized by vortex vigorously. The homogenized sample was then transferred to a −20 °C freezer for storage prior to genomic DNA and total RNA extraction.

Fecal Total RNA Extraction. Total fecal RNA was extracted by using a TRIzol-based method. Briefly, 300 μL of homogenized fecal sample (in shield buffer), 900 μL of TRIzol reagent (ThermoFisher 15596018), and 0.2 ng ERCC RNA Spike-In Mix (ThermoFisher 4456740) were added to a RNase-free Eppendorf 1.5 mL tube, and the sample was then fully homogenized by vortexing vigorously and incubated at room temperature for 15 min to ensure total RNA was fully released. Next, the tube was centrifuged at 12,000 × *g* for 10 min at 4 °C, and debris-free supernatant was transferred to a new RNase-free Eppendorf 1.5 mL tube. Next, fecal total RNA was extracted using Direct-zol RNA purification kits (Zymo R2054) according to the manufacturer's instructions, and the final yield was quantified using Qubit RNA HS Assay (ThermoFisher Q32855).

Amplicon Primer Design for Multiplex PCR. Primers used in multiplex PCR reaction were designed by PrimerQuest (Integrated DNA Technologies)[57] and optimized by SADDLE algorithm.[58] Briefly, the cDNA sequences of most dominant transcripts of selected gene targets were obtained from the Ensembl genome database (mouse: GRCm39) and primer pair candidates of each transcript were designed using the online service of PrimerQuest with the following criteria settings: Primer Tm: 62−66 °C (Opt: 64 °C); Primer GC: 35% to 65% (Opt: 50%); Primer size: 20 nt to 30 nt (Opt: 24 nt); Amplicon size: 320 bp to 380 bp. Top 5 designs of each transcript were then subjected to optimized selection by performing the SADDLE algorithm to minimize the potential of primer dimer formation. Illumina adapter, 6 nt unique amplicon identifier (UAI) and 6 nt linker sequences were then added to the 5′ of selected primer sets, and the final primers used in multiplex PCR reactions were synthesized as oligo pools by Integrated DNA Technologies. Sequences of primers used in multiplex PCR reactions are provided in Table S2.

Stool-based Host Cell Sequencing and Library Preparation. Total RNA extracted from feces was first subjected to genomic DNA removal by TURBO DNase. Briefly, a 30 μL digestion reaction was set up with 400 ng mouse fecal RNA as input and incubated at 37 °C for 20 min on a thermocycler. Next, genomic DNA-free RNA was purified by 2× AMPure XP beads (Beckman−Coulter A63881) following the manufacturer's instruction and eluted into 12 μL of nuclease-free water. Then, cDNA was generated by SuperScript IV First-Strand Synthesis System (ThermoFisher 18091200) following the manufacturer's instruction with random hexamer, oligo dT, and 11 μL purified RNA as input, then yielding cDNA was purified by 2× AMPure XP beads again and eluted in 10 μL nuclease-free water. Subsequently, a 10 μL multiplex PCR reaction was set up with 5 μL of cDNA as template, 2 μL of multiplex PCR 5× master mix (NEB M0284S), and 0.2 μL of DMSO and primers mix (5 nM final concentration per primer). The amplicon generation reaction was run on a thermocycler with limited cycles: (95 °C 2 min; 14 cycles: 95 °C 30 s, 61 °C 30 s, 68 °C 60 s; 65 °C 5 min; 4 °C infinite). Then, the yielding amplicon product was subjected to 0.9× SPRIselect beads cleanup (Beckman−Coulter B23318) and Exonuclease I digestion (NEB M0293S) to remove leftover primers. Finally, Illumina P5 and P7 index adapters were added to the amplicons by additional PCR amplification: a 40 μL amplification reaction (10 μL purified amplicons, 2.5 μL 10 μM P5 index primer, 2.5 μL 10 μM P7 index primer, 20 μL KAPA HiFi HotStart ReadyMix (Roche KK2602) and 5 μL nuclease-free water) was run on a thermocycler with following program: (98 °C 3 min, 35 cycles: 98 °C 20 s, 67 °C 15 s, 72 °C 60 s; 72 °C 5 min; 4 °C infinite). The final library products were then subjected to 2% gel electrophoresis, and expected DNA bands (480 to 540 bp) were excised from gel and extracted by Monarch DNA gel extraction kit (NEB T1020S) following the manufacturer's instructions. Gel-purified libraries were quantified by Qubit dsDNA HS assay (Thermo Q32851) and sequenced on Illumina NextSeq platform (HO150, 2 × 75 paired-end mode) with 15% PhiX spike-in (Illumina FC-110-3001) following the manufacturer's instructions. Sequences of primers used in library preparation are provided in Table S2.

Sequencing Data Analysis. Raw sequencing reads were first processed using Cutadapt v2.1[59] with following parameters "-a AGATCGGAAGAGCACACGTC -A AGATCGGAAGAGCGTCGTGT --discard-trimmed --trim-n -q 15 --pair-filter = any --max-n 0" to remove any adapter-containing reads generated from primer dimer in multiplex PCR reaction. Next, unique amplicon identifier (UAI) sequences were extracted, and the first 35 bp of reads were trimmed to avoid alignment artifacts. Remaining part of reads were the aligned to reference cDNA sequences used in amplicon primer design by Bowtie2[60] in "--very-sensitive" mode and reads counts of each transcript were calculated based on concordantly aligned reads pairs. Relative abundances of host transcripts (reads per thousand mapped reads) in each sample were defined as UAI counts of specific transcripts normalized by the sum of UAI counts of all host transcripts in the sample, and absolute amounts of exfoliated RNA (biomass) were defined as the sum of UAI counts of all host transcripts normalized by weights of feces and sum of UAI counts of ERCC spike-in. Differential gene expression analysis was carried out using DESeq2.[61] Differential gene expression was defined as >2-fold change in gene expression relative to Day 0, with Padj < 0.05. *p* values of differential expression were all adjusted using the Benjamini−Hochberg procedure in DESeq2 using default settings.

Microbial Genomic DNA Extraction. Genomic DNA (gDNA) of mouse gut microbes were extracted from feces using a silica bead beating-based protocol adapted from Ji et al.[62] Briefly, 200 μL of 0.1 mm Zirconia Silica beads (Biospec 11079101Z), 600 μL of lysis solution (50 mM Tris-HCl pH7.5 and 0.2 mM EDTA), 200 μL of homogenized feces in shield buffer, and 1 μL of saturated culture of spike-in strain (*Sporosarcina pasteurii* (ATCC 11859)) were added to each well of a 96-well 2 mL plates (Fisher 07-202-505). The plate was then covered by a bead sealing mat (Axygen AM-2 ML-RD) and subjected to bead beating for 5 min on a bead beater (Biospec 1001) followed by a 10 min cooling period. The bead beating cycle was repeated once and plates were centrifuged at 4500 × *g* for 5 min to spin down cell debris. Next, 60 μL cell lysate was transferred to a new plate and 15 μL proteinase K

https://doi.org/10.1021/acssynbio.4c00453
ACS Synth. Biol. 2024, 13, 4002−4014

solution (50 mM Tris-HCl pH7.5 and 1 μg/μL proteinase K (Lucigen MPRK092)) was added. The mixed solution was subjected to proteinase K digestion on a thermal cycler (65 °C 30 min, 95 °C 30 min, 4 °C infinite) and subsequently purified by 1× Ampure XP SPRI beads cleanup (Beckman-Coulter A63881) following the manufacturer's instructions to yield final gDNA.

16S rRNA Sequencing. Sequencing of the 16S hypervariable region 4 (V4) region was performed utilizing a custom dual-indexing protocol, detailed fully in Ji et al.[62] Briefly, a 20 μL 16S−V4 amplification reaction was set up with 2 μL extracted gDNA as template and barcoded primers. Next, a quantitative amplification was performed (98 °C 30 s, cycles: 98 °C 10 s, 55 °C 20 s, 65 °C 60 s; 65 °C 5 min; 4 °C infinite) and stopped during exponential phase (typically 13−15 cycles), and the reaction was advanced to the final extension step. The resulting amplicon libraries were normalized and pooled based on fluorescence Intensity and subjected to gel electrophoresis to excise expected DNA bands (~390bp). Gel-purified libraries were quantified by Qubit dsDNA HS assay (Thermo Q32851) and sequenced on Illumina MiSeq platform (reagent kits: v2 300 cycles, paired-end mode) at 8 pM loading concentration with 25% PhiX spike-in (Illumina FC-110-3001) along with custom sequencing primers spiked into MiSeq reagent cartridge following the manufacturer's instructions.

16S rRNA Data Analysis. Raw sequencing reads of 16S−V4 amplicon were analyzed by USEARCH v11.0.667.[63] Specifically, paired-end reads were merged using "-fastq_mergepairs" mode with the default setting. Merged reads were then subjected to quality filtering using "-fastq_filter" mode with the option "-fastq_maxee 1.0 -fastq_minlen 240". Remaining reads were deduplicated (-fastx_uniques) and clustered into operational taxonomic units (OTUs) (-cluster_otus) at 97% identity with the option "-minsize 2", and merged reads were then searched against OTU sequences (−otutab) to generate an OTU count table. Taxonomy of OTUs were assigned using Ribosomal Database Project classifier v2.13 trained with 16S rRNA training set 18.[64] Relative abundances were defined as read counts of specific OTU normalized by total number of nonspike-in reads, and absolute abundances were defined as reads count of specific OTU normalized by weight of input feces and reads count of spike-in strain OTU. Alpha diversity was calculated based on the relative abundance of OTUs using "diversity()" function from the "vegan" package in R. Pairwise Bray−Curtis similarity was calculated between fecal samples from all mice before and after cage normalization (day −7, day 0). The distribution of pairwise distances was plotted at each time point using ggplot2 and compared using the Wilcoxon rank sum test.

GI Motility and *In Vivo* Metabolite Statistical Analyses. Group means, fold change, and standard errors/deviations were calculated in Microsoft Excel. For statistical significance, samples compared using one-way ANOVA on ranks (Kruskal−Wallis test with Dunn's test for multiple comparisons) ordinary were performed with plotted statistical values using ANOVA multiple comparisons in Graphpad Prism. Comparisons of two conditions were compared using the Mann−Whitney test in Graphpad Prism. A value of $p < 0.05$ was considered significant and p values marked in corresponding texts and figures (*$p < 0.05$, **$p < 0.01$, ***$p < 0.001$, and ****$p < 0.0001$). Error bars represent standard deviation, unless otherwise noted.

■ ASSOCIATED CONTENT

Data Availability Statement

All sequencing data generated in this study have been submitted to the NCBI BioProject database (http://www.ncbi.nlm.nih.gov/bioproject/) under accession number PRJNA1156177.

Supporting Information

The Supporting Information is available free of charge at https://pubs.acs.org/doi/10.1021/acssynbio.4c00453.

Design and *in vitro* characterization and optimization of 5-HT production in engineered strains; microbial localization throughout GI tract; serotonin supplementation modulates host gastrointestinal motility in a time-of-day dependent manner; temporal transcriptomic changes per treatment group; analysis of composition and diversity of fecal microbiome during *in vivo* studies (PDF)

Strains, plasmids, genes, and RBS variants used in this study (XLSX)

Primers used in this study (XLSX)

■ AUTHOR INFORMATION

Corresponding Authors

Morten O. A. Sommer − *Novo Nordisk Foundation Center for Biosustainability, Technical University of Denmark, Lyngby DK 2800, Denmark;* orcid.org/0000-0003-4005-5674; Email: msom@bio.dtu.dk

Harris H. Wang − *Department of Systems Biology, Columbia University Irving Medical Center, New York, New York 10032, United States; Department of Pathology and Cell Biology, Columbia University Irving Medical Center, New York, New York 10032, United States;* orcid.org/0000-0003-2164-4318; Email: harris.wang@columbia.edu

Authors

Chrystal F. Mavros − *Department of Systems Biology, Columbia University Irving Medical Center, New York, New York 10032, United States; Department of Genetics and Development, Columbia University Irving Medical Center, New York, New York 10032, United States;* orcid.org/0000-0003-3914-7512

Mareike Bongers − *Novo Nordisk Foundation Center for Biosustainability, Technical University of Denmark, Lyngby DK 2800, Denmark*

Frederik B. F. Neergaard − *Novo Nordisk Foundation Center for Biosustainability, Technical University of Denmark, Lyngby DK 2800, Denmark*

Frank Cusimano − *Department of Systems Biology, Columbia University Irving Medical Center, New York, New York 10032, United States; Department of Nutritional and Metabolic Biology, Columbia University Irving Medical Center, New York, New York 10032, United States*

Yiwei Sun − *Department of Systems Biology, Columbia University Irving Medical Center, New York, New York 10032, United States; Department of Biomedical Informatics, Columbia University Irving Medical Center, New York, New York 10032, United States*

Andrew Kaufman − *Department of Systems Biology, Columbia University Irving Medical Center, New York, New York 10032, United States*

Miles Richardson − *Department of Systems Biology, Columbia University Irving Medical Center, New York, New York 10032, United States*
Susanne Kammler − *Novo Nordisk Foundation Center for Biosustainability, Technical University of Denmark, Lyngby DK 2800, Denmark*
Mette Kristensen − *Novo Nordisk Foundation Center for Biosustainability, Technical University of Denmark, Lyngby DK 2800, Denmark*

Complete contact information is available at: https://pubs.acs.org/10.1021/acssynbio.4c00453

Author Contributions

[▽]C.F.M., M.B., and F.B.F.N. contributed equally. C.F.M., M.B., F.B.F.N. M.O.A.S., S.K., and H.H.W. designed the study. C.F.M., M.B., F.B.F.N., and A.K. performed the experiments and analyzed the data with input from M.O.A.S. and H.H.W. 16S and gene expression results were analyzed by Y.S. and M.R. Immunohistochemistry experiments were performed by F.C. M.K. provided analytical methods for strain generation. The manuscript was written by C.F.M., M.B., F.B.F.N., and H.H.W. with input from all authors.

Notes

The authors declare the following competing financial interest(s): A provisional patent application has been filed by The Trustees of Columbia University in the City of New York and Technical University of Denmark based on this work. H.H.W. is a scientific advisor of SNIPR Biome, Kingdom Supercultures, Fitbiomics, VecX Biomedicines, Genus PLC, and a scientific co-founder of Aclid and Foli Bio, all of whom are not involved in the study. The authors declare no additional competing financial interests.

■ ACKNOWLEDGMENTS

We are very grateful to Michael Gershon for helpful scientific discussions and feedback. We thank Hao Luo, Markus Herrgård, Rebecca Lennen, and Se Hyeuk Kim from the NNF Center for Biosustainability Translational Core for advice on strain construction, as well as Rasmus Wied Pedersen for help with *in vitro* experiments. H.H.W. acknowledges funding from AFOSR (UES S-168-4X5-001), ONR (N00014-15-1-2704), NIH (2R01AI132403, 1R01DK118044, 1R01EB031935, 1R21AI146817-01), NSF (MCB-2025515), the Hirschl Trust (HRSCHLCU19-3823), and Burroughs Wellcome Fund (PATH1016691) for this work. M.B., F.B.F.N, S.K., and M.O.A.S. acknowledge funding from The Novo Nordisk Foundation (NNF) (NNF10CC1016517 and NNF20CC0035580), the NNF Challenge program CaMiT (NNF17CO0028232), and from the BioInnovation Institute (NNF20SA0059386 and BII21SG1020354).

■ REFERENCES

(1) Gilbert, J. A.; Blaser, M. J.; Caporaso, J. G.; Jansson, J. K.; Lynch, S. V.; Knight, R. Current Understanding of the Human Microbiome. *Nat. Med.* **2018**, *24* (4), 392−400.
(2) Dinan, T. G.; Cryan, J. F. Brain-Gut-Microbiota Axis and Mental Health. *Psychosom. Med.* **2017**, *79* (8), 920−926.
(3) Suez, J.; Zmora, N.; Segal, E.; Elinav, E. The Pros, Cons, and Many Unknowns of Probiotics. *Nat. Med.* **2019**, *25* (5), 716−729.
(4) SpringerMicrobial Endocrinology: The Microbiota-Gut-Brain Axis in Health and Disease*Advances in Experimental Medicine and Biology*Lyte, M.; Cryan, J. F.SpringerNew York, NY2014Vol. *817*.
(5) Bangsgaard Bendtsen, K. M.; Krych, L.; Sørensen, D. B.; Pang, W.; Nielsen, D. S.; Josefsen, K.; Hansen, L. H.; Sørensen, S. J.; Hansen, A. K. Gut Microbiota Composition Is Correlated to Grid Floor Induced Stress and Behavior in the BALB/c Mouse. *PLoS One* **2012**, *7* (10), No. e46231.
(6) Madison, A.; Kiecolt-Glaser, J. K. Stress Depression, Diet, and the Gut Microbiota: Human−Bacteria Interactions at the Core of Psychoneuroimmunology and Nutrition. *Curr. Opin. Behav. Sci.* **2019**, *28*, 105−110.
(7) Aguilera, M.; Vergara, P.; Martínez, V. Stress and Antibiotics Alter Luminal and Wall-adhered Microbiota and Enhance the Local Expression of Visceral Sensory-related Systems in Mice. *Neurogastroenterol. Motil.* **2013**, *25* (8), No. e515-e529.
(8) Gershon, M. D. 5-Hydroxytryptamine (Serotonin) in the Gastrointestinal Tract. *Curr. Opin. Endocrinol., Diabetes Obes* **2013**, *20* (1), 14−21.
(9) Koopman, N.; Katsavelis, D.; Ten Hove, A.; Brul, S.; de Jonge, W.; Seppen, J. The Multifaceted Role of Serotonin in Intestinal Homeostasis. *Int. J. Mol. Sci.* **2021**, *22* (17), 9487.
(10) Goldstein, B. J.; Goodnick, P. J. Selective Serotonin Reuptake Inhibitors in the Treatment of Affective Disorders—III. Tolerability, Safety and Pharmacoeconomics. *J. Psychopharmacol.* **1998**, *12* (4_suppl), 55−S87.
(11) Ferguson, J. M. SSRI Antidepressant Medications: Adverse effects and tolerability. *Prim. Care Companion CNS Disord* **2001**, *3* (1), 22−27.
(12) Mandić, A. D.; Woting, A.; Jaenicke, T.; Sander, A.; Sabrowski, W.; Rolle-Kampcyk, U.; von Bergen, M.; Blaut, M. Clostridium Ramosum Regulates Enterochromaffin Cell Development and Serotonin Release. *Sci. Rep.* **2019**, *9* (1), 1177.
(13) Yano, J. M.; Yu, K.; Donaldson, G. P.; Shastri, G. G.; Ann, P.; Ma, L.; Nagler, C. R.; Ismagilov, R. F.; Mazmanian, S. K.; Hsiao, E. Y. Indigenous Bacteria from the Gut Microbiota Regulate Host Serotonin Biosynthesis. *Cell* **2015**, *161* (2), 264−276.
(14) Hara, T.; Mihara, T.; Ishibashi, M.; Kumagai, T.; Joh, T. Heat-Killed Lactobacillus Casei Subsp. Casei 327 Promotes Colonic Serotonin Synthesis in Mice. *J. Funct. Foods* **2018**, *47*, 585−589.
(15) Sanidad, K. Z.; Rager, S. L.; Carrow, H. C.; Ananthanarayanan, A.; Callaghan, R.; Hart, L. R.; Li, T.; Ravisankar, P.; Brown, J. A.; Amir, M.; et al. Gut Bacteria−Derived Serotonin Promotes Immune Tolerance in Early Life. *Sci. Immunol.* **2024**, *9* (93), No. eadj4775.
(16) Li, B.; Li, M.; Luo, Y.; Li, R.; Li, W.; Liu, Z. Engineered 5-HT Producing Gut Probiotic Improves Gastrointestinal Motility and Behavior Disorder. *Front. Cell. Infect. Microbiol.* **2022**, *12*, 1013952.
(17) Riglar, D. T.; Silver, P. A. Engineering Bacteria for Diagnostic and Therapeutic Applications. *Nat. Rev. Microbiol.* **2018**, *16* (4), 214−225.
(18) Huang, Y.; Lin, X.; Yu, S.; Chen, R.; Chen, W. Intestinal Engineered Probiotics as Living Therapeutics: Chassis Selection, Colonization Enhancement, Gene Circuit Design, and Biocontainment. *ACS Synth. Biol.* **2022**, *11* (10), 3134−3153.
(19) Riglar, D. T.; Giessen, T. W.; Baym, M.; Kerns, S. J.; Niederhuber, M. J.; Bronson, R. T.; Kotula, J. W.; Gerber, G. K.; Way, J. C.; Silver, P. A. Engineered Bacteria Can Function in the Mammalian Gut Long-Term as Live Diagnostics of Inflammation. *Nat. Biotechnol.* **2017**, *35* (7), 653−658.
(20) Mao, N.; Cubillos-Ruiz, A.; Cameron, D. E.; Collins, J. J. Probiotic Strains Detect and Suppress Cholera in Mice. *Sci. Transl. Med.* **2018**, *10* (445), No. eaao2586.
(21) Daeffler, K. N.; Galley, J. D.; Sheth, R. U.; Ortiz-Velez, L. C.; Bibb, C. O.; Shroyer, N. F.; Britton, R. A.; Tabor, J. J. Engineering Bacterial Thiosulfate and Tetrathionate Sensors for Detecting Gut Inflammation. *Mol. Syst. Biol.* **2017**, *13* (4), 923.
(22) Mimee, M.; Nadeau, P.; Hayward, A.; Carim, S.; Flanagan, S.; Jerger, L.; Collins, J.; McDonnell, S.; Swartwout, R.; Citorik, R. J.; Bulović, V.; Langer, R.; Traverso, G.; Chandrakasan, A. P.; Lu, T. K. An Ingestible Bacterial-Electronic System to Monitor Gastrointestinal Health. *Science* **2018**, *360* (6391), 915−918.

(23) Saeidi, N.; Wong, C. K.; Lo, T.; Nguyen, H. X.; Ling, H.; Leong, S. S. J.; Poh, C. L.; Chang, M. W. Engineering Microbes to Sense and Eradicate *Pseudomonas Aeruginosa*, a Human Pathogen. *Mol. Syst. Biol.* **2011**, *7* (1), 521.
(24) Isabella, V. M.; Ha, B. N.; Castillo, M. J.; Lubkowicz, D. J.; Rowe, S. E.; Millet, Y. A.; Anderson, C. L.; Li, N.; Fisher, A. B.; West, K. A.; Reeder, P. J.; Momin, M. M.; Bergeron, C. G.; Guilmain, S. E.; Miller, P. F.; Kurtz, C. B.; Falb, D. Development of a Synthetic Live Bacterial Therapeutic for the Human Metabolic Disease Phenylketonuria. *Nat. Biotechnol.* **2018**, *36* (9), 857−864.
(25) Kurtz, C. B.; Millet, Y. A.; Puurunen, M. K.; Perreault, M.; Charbonneau, M. R.; Isabella, V. M.; Kotula, J. W.; Antipov, E.; Dagon, Y.; Denney, W. S.; Wagner, D. A.; West, K. A.; Degar, A. J.; Brennan, A. M.; Miller, P. F. An Engineered *E. Coli* Nissle Improves Hyperammonemia and Survival in Mice and Shows Dose-Dependent Exposure in Healthy Humans. *Sci. Transl. Med.* **2019**, *11* (475), No. eaau7975.
(26) Duan, F. F.; Liu, J. H.; March, J. C. Engineered Commensal Bacteria Reprogram Intestinal Cells Into Glucose-Responsive Insulin-Secreting Cells for the Treatment of Diabetes. *Diabetes* **2015**, *64* (5), 1794−1803.
(27) Steidler, L.; Hans, W.; Schotte, L.; Neirynck, S.; Obermeier, F.; Falk, W.; Fiers, W.; Remaut, E. Treatment of Murine Colitis by Lactococcus Lactis Secreting Interleukin-10. *Science* **2000**, *289*, 1352−1355.
(28) Park, S.; Kang, K.; Lee, S. W.; Ahn, M.-J.; Bae, J.-M.; Back, K. Production of Serotonin by Dual Expression of Tryptophan Decarboxylase and Tryptamine 5-Hydroxylase in *Escherichia Coli*. *Appl. Microbiol. Biotechnol.* **2011**, *89* (5), 1387−1394.
(29) Mora-Villalobos, J.-A.; Zeng, A.-P. Synthetic Pathways and Processes for Effective Production of 5-Hydroxytryptophan and Serotonin from Glucose in *Escherichia Coli*. *J. Biol. Eng.* **2018**, *12* (1), 3.
(30) Sonnenborn, U. *Escherichia Coli*Strain Nissle 1917—from Bench to Bedside and Back: History of a Special*Escherichia Coli*Strain with Probiotic Properties. *FEMS Microbiol. Lett.* **2016**, *363* (19), fnw212.
(31) Hägg, P.; de Pohl, J. W.; Abdulkarim, F.; Isaksson, L. A. A Host/Plasmid System That Is Not Dependent on Antibiotics and Antibiotic Resistance Genes for Stable Plasmid Maintenance in *Escherichia Coli*. *J. Biotechnol.* **2004**, *111* (1), 17−30.
(32) Blum-Oehler, G.; Oswald, S.; Eiteljörge, K.; Sonnenborn, U.; Schulze, J.; Kruis, W.; Hacker, J. Development of Strain-Specific PCR Reactions for the Detection of the Probiotic *Escherichia Coli* Strain Nissle 1917 in Fecal Samples. *Res. Microbiol.* **2003**, *154* (1), 59−66.
(33) Gerdes, K.; Gultyaev, A. P.; Franch, T.; Pedersen, K.; Mikkelsen, N. D. Antisense RNA-regulated programmed cell death. *Annu. Rev. Genet.* **1997**, *31* (1), 1−31.
(34) Back, K.; Tan, D.; Reiter, R. J. Melatonin Biosynthesis in Plants: Multiple Pathways Catalyze Tryptophan to Melatonin in the Cytoplasm or Chloroplasts. *J. Pineal Res.* **2016**, *61* (4), 426−437.
(35) Dubouzet, J. G.; Matsuda, F.; Ishihara, A.; Miyagawa, H.; Wakasa, K. Production of Indole Alkaloids by Metabolic Engineering of the Tryptophan Pathway in Rice. *Plant Biotechnol. J.* **2013**, *11* (9), 1103−1111.
(36) Mano, Y.; Nemoto, K. The Pathway of Auxin Biosynthesis in Plants. *J. Exp. Bot.* **2012**, *63* (8), 2853−2872.
(37) Luo, H.; Yang, L.; Kim, S. H.; Wulff, T.; Feist, A. M.; Herrgard, M.; Palsson, B. Ø. Directed Metabolic Pathway Evolution Enables Functional Pterin-Dependent Aromatic-Amino-Acid Hydroxylation in *Escherichia Coli*. *ACS Synth. Biol.* **2020**, *9* (3), 494−499.
(38) Schramek, N.; Bracher, A.; Fischer, M.; Auerbach, G.; Nar, H.; Huber, R.; Bacher, A. Reaction Mechanism of GTP Cyclohydrolase I: Single Turnover Experiments Using a Kinetically Competent Reaction Intermediate1. *J. Mol. Biol.* **2002**, *316* (3), 829−837.
(39) Windahl, M. S.; Boesen, J.; Karlsen, P. E.; Christensen, H. E. M. Expression, Purification and Enzymatic Characterization of the Catalytic Domains of Human Tryptophan Hydroxylase Isoforms. *Protein J.* **2009**, *28* (9−10), 400−406.
(40) Bhattarai, Y.; Williams, B. B.; Battaglioli, E. J.; Whitaker, W. R.; Till, L.; Grover, M.; Linden, D. R.; Akiba, Y.; Kandimalla, K. K.; Zachos, N. C.; et al. Gut Microbiota-Produced Tryptamine Activates an Epithelial G-Protein-Coupled Receptor to Increase Colonic Secretion. *Cell Host Microbe* **2018**, *23* (6), 775−785.e5.
(41) Terry, N.; Margolis, K. G.Serotonergic Mechanisms Regulating the GI Tract: Experimental Evidence and Therapeutic Relevance In *Gastrointestinal Pharmacology*. Greenwood-Van Meerveld, B. ed.; Springer International Publishing: Cham 2017, pp. 319−342, .
(42) Gershon, M. D. Nerves, Reflexes, and the Enteric Nervous System. *J. Clin. Gastroenterol.* **2005**, *39* (5), S184−S193.
(43) Fida, R.; Bywater, R. A. R.; Lyster, D. J. K.; Taylor, G. S. Chronotropic Action of 5-Hydroxytryptamine (5-HT) on Colonic Migrating Motor Complexes (CMMCs) in the Isolated Mouse Colon. *J. Auton. Nerv. Syst.* **2000**, *80* (1−2), 52−63.
(44) Fung, T. C.; Vuong, H. E.; Luna, C. D. G.; Pronovost, G. N.; Aleksandrova, A. A.; Riley, N. G.; Vavilina, A.; McGinn, J.; Rendon, T.; Forrest, L. R.; Hsiao, E. Y. Intestinal Serotonin and Fluoxetine Exposure Modulate Bacterial Colonization in the Gut. *Nat. Microbiol.* **2019**, *4* (12), 2064−2073.
(45) Herr, N.; Bode, C.; Duerschmied, D. The Effects of Serotonin in Immune Cells. *Front. Cardiovasc. Med.* **2017**, *4*, 48.
(46) Bellono, N. W.; Bayrer, J. R.; Leitch, D. B.; Castro, J.; Zhang, C.; O'Donnell, T. A.; Brierley, S. M.; Ingraham, H. A.; Julius, D. Enterochromaffin Cells Are Gut Chemosensors That Couple to Sensory Neural Pathways. *Cell* **2017**, *170* (1), 185−198.e16.
(47) Wei, L.; Singh, R.; Ghoshal, U. C. Enterochromaffin Cells−Gut Microbiota Crosstalk: Underpinning the Symptoms, Pathogenesis, and Pharmacotherapy in Disorders of Gut-Brain Interaction. *J. Neurogastroenterol. Motil.* **2022**, *28* (3), 357−375.
(48) Han, N. D.; Cheng, J.; Delannoy-Bruno, O.; Webber, D.; Terrapon, N.; Henrissat, B.; Rodionov, D. A.; Arzamasov, A. A.; Osterman, A. L.; Hayashi, D. K.; et al. Microbial Liberation of N-Methylserotonin from Orange Fiber in Gnotobiotic Mice and Humans. *Cell* **2022**, *185* (16), 3056−3057.
(49) Rozenblit-Susan, S.; Chapnik, N.; Froy, O. Serotonin Prevents Differentiation of Brown Adipocytes by Interfering with Their Clock. *Obesity* **2019**, *27* (12), 2018−2024.
(50) Hoffman, J. M.; Tyler, K.; MacEachern, S. J.; Balemba, O. B.; Johnson, A. C.; Brooks, E. M.; Zhao, H.; Swain, G. M.; Moses, P. L.; Galligan, J. J.; et al. Activation of Colonic Mucosal 5-HT4 Receptors Accelerates Propulsive Motility and Inhibits Visceral Hypersensitivity. *Gastroenterology* **2012**, *142* (4), 844−854.e4.
(51) Spohn, S. N.; Bianco, F.; Scott, R. B.; Keenan, C. M.; Linton, A. A.; O'Neill, C. H.; Bonora, E.; Dicay, M.; Lavoie, B.; Wilcox, R. L.; et al. Protective Actions of Epithelial 5-Hydroxytryptamine 4 Receptors in Normal and Inflamed Colon. *Gastroenterology* **2016**, *151* (5), 933−944.e3.
(52) Rachdi, L.; Zhou, Z.; Berthault, C.; Lourenço, C.; Fouque, A.; Domet, T.; Armanet, M.; You, S.; Peakman, M.; Mallone, R.; Scharfmann, R. Tryptophan Metabolism Promotes Immune Evasion in Human Pancreatic β Cells. *eBiomedicine* **2023**, *95*, 104740.
(53) Urtecho, G.; Moody, T.; Huang, Y.; Sheth, R. U.; Richardson, M.; Descamps, H. C.; Kaufman, A.; Lekan, O.; Velez-Cortes, F.; Qu, Y. Spatiotemporal Dynamics during Niche Remodeling by Super-Colonizing Microbiota in the Mammalian Gut. *bioRxiv* **2022**, 2022−10.
(54) Grondin, J. A.; Khan, W. I. Emerging Roles of Gut Serotonin in Regulation of Immune Response, Microbiota Composition and Intestinal Inflammation. *J. Can. Assoc. Gastroenterol.* **2024**, *7* (1), 88−96.
(55) Minderhoud, I. M.; Oldenburg, B.; Schipper, M. E. I.; ter Linde, J. J. M.; Samsom, M. Serotonin Synthesis and Uptake in Symptomatic Patients With Crohn's Disease in Remission. *Clin. Gastroenterol. Hepatol.* **2007**, *5* (6), 714−720.
(56) Abdala-Valencia, H.; Berdnikovs, S.; McCary, C. A.; Urick, D.; Mahadevia, R.; Marchese, M. E.; Swartz, K.; Wright, L.; Mutlu, G. M.; Cook-Mills, J. M. Inhibition of Allergic Inflammation by Supple-

https://doi.org/10.1021/acssynbio.4c00453
ACS Synth. Biol. 2024, 13, 4002−4014

mentation with 5-Hydroxytryptophan. *Am. J. Physiol. Lung Cell. Mol. Physiol.* **2012**, *303* (8), L642−L660.
(57) Owczarzy, R.; Tataurov, A. V.; Wu, Y.; Manthey, J. A.; McQuisten, K. A.; Almabrazi, H. G.; Pedersen, K. F.; Lin, Y.; et al. IDT SciTools: A Suite for Analysis and Design of Nucleic Acid Oligomers. *Nucleic Acids Res.* **2008**, *36*, W163−W169.
(58) Xie, N. G.; Wang, M. X.; Song, P.; Mao, S.; Wang, Y.; Yang, Y.; Luo, J.; Ren, S.; Zhang, D. Y. Designing Highly Multiplex PCR Primer Sets with Simulated Annealing Design Using Dimer Likelihood Estimation (SADDLE). *Nat. Commun.* **2022**, *13* (1), 1881.
(59) Martin, M. Cutadapt Removes Adapter Sequences from High-Throughput Sequencing Reads. *EMBnet J.* **2011**, *17* (1), 10.
(60) Langmead, B.; Salzberg, S. L. Fast Gapped-Read Alignment with Bowtie 2. *Nat. Methods* **2012**, *9* (4), 357−359.
(61) Love, M. I.; Huber, W.; Anders, S. Moderated Estimation of Fold Change and Dispersion for RNA-Seq Data with DESeq2. *Genome Biol.* **2014**, *15* (12), 550.
(62) Ji, B. W.; Sheth, R. U.; Dixit, P. D.; Huang, Y.; Kaufman, A.; Wang, H. H.; Vitkup, D. Quantifying Spatiotemporal Variability and Noise in Absolute Microbiota Abundances Using Replicate Sampling. *Nat. Methods* **2019**, *16* (8), 731−736.
(63) Edgar, R. C. Search and Clustering Orders of Magnitude Faster than BLAST. *Bioinformatics* **2010**, *26* (19), 2460−2461.
(64) Wang, Q.; Garrity, G. M.; Tiedje, J. M.; Cole, J. R. Naïve Bayesian Classifier for Rapid Assignment of rRNA Sequences into the New Bacterial Taxonomy. *Appl. Environ. Microbiol.* **2007**, *73* (16), 5261−5267.

https://doi.org/10.1021/acssynbio.4c00453
ACS Synth. Biol. 2024, 13, 4002−4014